DISCRETE AND CONTINUOUS
DYNAMICAL SYSTEMS SERIES B
Volume **17**, Number **8**, November **2012**

doi:10.3934/dcdsb.2012.17.2815

pp. **2815–2827**

VEGETATION PATTERNS AND DESERTIFICATION WAVES IN SEMI-ARID ENVIRONMENTS: MATHEMATICAL MODELS BASED ON LOCAL FACILITATION IN PLANTS

Jonathan A. Sherratt and Alexios D. Synodinos

Department of Mathematics and Maxwell Institute for Mathematical Sciences
Heriot-Watt University
Edinburgh EH14 4AS, UK

Abstract. In semi-arid regions, infiltration of rain water into the soil is significantly higher in vegetated areas than for bare ground. However, quantitative data on the dependence of infiltration capacity on plant biomass is very limited. In this paper, we use a simple reaction-diffusion-advection model to investigate the effects of varying the strength of this dependence. We begin by studying the formation of banded vegetation patterns on gentle slopes ("tiger bush"), which is a hallmark of semi-deserts. We calculate the range of rainfall parameter values over which such patterns occur, using numerical continuation methods. We then consider interfaces between vegetation and bare ground, showing that the vegetated region either expands or contracts depending on whether the rainfall parameter is above or below a critical value. We conclude by discussing the mathematical questions raised by our work.

1. **Introduction.** Water is the limiting resource for plants in semi-arid environments. In many such ecosystems there is strong evidence that the infiltration of rain water into the soil is positively correlated with vegetation biomass [6, 20, 33, 48]. On bare ground, much of the water that falls as rain simply runs off, but higher levels of organic matter in the soil, and the presence of roots, increases the proportion of rain water infiltrating into the soil. This results in a greater water availability, and thus increased plant growth, when vegetation biomass is larger. This local facilitation is widely regarded as a key mechanism underlying the vegetation patterning that is common in semi-arid environments (see [1, 35, 48] for review). Such patterns are typically mosaics on flat terrain and stripes running parallel to the contours on slopes, and consist of vegetated regions separated by bare ground. Vegetation patterns are widespread in sub-Saharan Africa [7, 28, 49], Australia [4, 13], and Mexico/South-Western USA [29, 30]. The "water redistribution hypothesis" is that most rain falling on (almost) bare ground runs off to nearby vegetated regions, where infiltration rates are higher, promoting further plant growth. However, it is important to note that there are other hypothesised mechanisms for vegetation pattern formation in semi-arid environments. Most notably, a number of authors have stressed the role of non-locality of water uptake due to extended root systems,

2000 *Mathematics Subject Classification.* Primary: 92B05; Secondary: 35K57, 35K65.

Key words and phrases. Pattern formation, mathematical model, arid landscapes, Brousse Tigrée, desert, travelling waves, wavetrain, plant cooperation.

JAS was supported in part by a Leverhulme Trust Research Fellowship.

either in conjunction with water redistribution (e.g. [17, 25, 52]) or in combination with local facilitation due to shading (e.g. [3, 26, 27]).

Mathematical modelling has been used extensively to study the water redistribution hypothesis. The first partial differential equation model was due to Klausmeier [24]; see [5, 18, 19, 23, 32, 34, 43, 45, 46, 47, 50] for examples of subsequent models. Klausmeier's model is expressed in terms of vegetation biomass $U(x,t)$ and water $W(x,t)$:

$$\begin{aligned} \partial U/\partial T &= \overbrace{k_1 UWF(U)}^{\text{plant growth}} - \overbrace{k_2 U}^{\text{plant loss}} + \overbrace{k_3\,\partial^2 U/\partial X^2}^{\text{dispersal}} && \text{(1a)}\\ \partial W/\partial T &= \underbrace{k_4}_{\text{rainfall}} - \underbrace{k_5 W}_{\text{evaporation}} - \underbrace{k_6 UWF(U)}_{\substack{\text{uptake}\\ \text{by plants}}} + \underbrace{k_7\,(\partial W/\partial X)}_{\substack{\text{flow}\\ \text{downhill}}}. && \text{(1b)} \end{aligned}$$

Here $k_1,\ldots,k_7$ are positive constants and the function $F(U)$ represents the dependence of infiltration on vegetation biomass. As discussed above, there is a large body of evidence that $F(.)$ is an increasing function in semi-arid ecosystems, but quantitative empirical data on which the form of $F(.)$ can be based is extremely limited. (See Figure 4 of [33] for one example of a relevant data set). Therefore Klausmeier [24] took $F(U)=U$, on the basis of mathematical simplicity rather than ecological data. Our objective is to study how model predictions change with the strength of the dependence of infiltration on vegetation biomass, and we consider specifically the one-parameter family of functional forms $F(U)=U^{p-1}$ with $p>1$.

Substituting the rescalings

$$\begin{gathered} u = Uk_6^{1/p}k_5^{-1/p} \quad w = Wk_1k_5^{-1/p}k_6^{-1+1/p} \quad x = Xk_5^{1/2}k_3^{-1/2} \quad t = Tk_5 \\ A = k_4k_1k_5^{-1-1/p}k_6^{-1+1/p} \quad B = k_2k_5^{-1} \quad \nu = k_7k_3^{-1/2}k_5^{-1/2}. \end{gathered} \tag{2}$$

into (1) with $F(U)=U^{p-1}$ gives the dimensionless system

$$\begin{aligned} \partial u/\partial t &= wu^p - Bu + \partial^2 u/\partial x^2 && \text{(3a)}\\ \partial w/\partial t &= A - w - wu^p + \nu\partial w/\partial x. && \text{(3b)} \end{aligned}$$

The parameters A, B and ν can be most usefully interpreted as corresponding to rainfall, plant loss (including herbivory) and slope gradient respectively, remembering that they actually depend on a combination of ecological quantities.

We will investigate the way in which the parameter p affects two different types of solution of (3): spatial patterns corresponding to banded vegetation on slopes (§2) and interfaces between homogeneous vegetation and bare ground on flat terrain (§3). In both cases, we will consider how the parameter p affects critical levels of rainfall at which there are qualitative changes in model solutions, namely the rainfall levels between which patterns occur, and the rainfall level at which the movement of interfaces changes direction. Before embarking on these studies, we draw attention to an important point regarding the parameters of the dimensional model (1): it is impossible to vary the parameter p while keeping the other dimensional parameters fixed. This is because when p changes, the values of k_1 and k_6 must also change, since their dimensions will change. Therefore it is not meaningful to ask how changing p affects a critical value of the (dimensional) rainfall parameter k_4, since one would also have to specify how k_1 and k_6 vary. In the nondimensional model (3), one can of course investigate how changes in p affect a critical value of A, but the results have

no direct interpretation in terms of rainfall due to the presence of p in the formula for A in (2). In view of these considerations, all of our results will be presented in terms of the changes with p of ratios of two critical values of A. These are the same as the ratios of the corresponding critical values of the dimensional rainfall parameter k_4.

2. **Vegetation patterns on slopes.** For all parameter values, (3) has a "desert" steady state $(u, w) = (0, A)$ that is stable. Steady states with $u \neq 0$ must satisfy

$$h(u) \equiv u + u^{1-p} = A/B \tag{4}$$

with $w = Bu^{1-p}$. Now $h(u) \to \infty$ as $u \to 0$ and ∞, with a unique local minimum at $u = u_{min} \equiv (p-1)^{1/p}$. Therefore there are zero or two solutions of (4) when A is $<$ or $> A_{crit} = Bh(u_{min}) = Bp(p-1)^{-1+1/p}$. Standard linear stability analysis shows that stability to homogeneous perturbations requires $u > u_{min}$ and $B < (1+u^p)/(p-1)$. The plant loss parameter B will vary between ecosystems but estimated values are all less than 1 [24, 34], and we will assume henceforth that $B < 1$. Then

$$u > u_{min} \Rightarrow \frac{1+u^p}{p-1} > \frac{1+u_{min}^p}{p-1} = \frac{p}{p-1} > 1 > B.$$

Thus the steady state with $u > u_{min}$ is stable to homogeneous perturbations, while that with $u < u_{min}$ is unstable.

We denote the first of these steady states by (u_s, w_s), so that $u_s > u_{min}$ and $w_s = Bu_s^{1-p}$. Patterns arise via (u_s, w_s) becoming unstable to inhomogeneous perturbations; an example of such a pattern is illustrated in Figure 1.

A natural approach to studying the conditions for pattern formation is to linearise (3) about (u_s, w_s) and then look for solutions proportional to $e^{ikx+\lambda t}$; patterns are expected when $\mathrm{Re}\,\lambda > 0$ for some $k \in \mathbb{R}$. This method was used in [38] for the original Klausmeier model ($p = 2$), but for general p the dispersion relation $\mathrm{Re}\,\lambda(k)$ is intractable. Therefore we must rely on a numerical study, for which we consider the full nonlinear equations (3).

The advection term in (3b) causes pattern solutions to move in the positive x direction (uphill). Ecologically, this migration has been the subject of a long controversy (see pp. 24-26 of [44] for a detailed discussion), but a large body of field data now supports the uphill migration of vegetation bands [8, 48], resulting from greater water availability near the upslope edge of a vegetation band than at the downslope edge. In view of this migration, the appropriate solution ansatz for patterns is $(u(x,t), w(x,t)) = (\widetilde{U}(z), \widetilde{W}(z))$, where $z = x - ct$ with $c > 0$ being the wave speed. Substituting this solution form into (3) gives

$$d^2\widetilde{U}/dz^2 + c\,d\widetilde{U}/dz + \widetilde{W}\widetilde{U}^p - B\widetilde{U} = 0 \tag{5a}$$

$$(\nu + c)d\widetilde{W}/dz + A - \widetilde{W} - \widetilde{W}\widetilde{U}^p = 0\,. \tag{5b}$$

Pattern solutions of (3) correspond to limit cycles of (5). We investigated these solutions using numerical continuation, implemented via the software package AUTO [10, 11, 12]. Fixing B, ν and c, we increased A from A_{crit} until (u_s, w_s) underwent a Hopf bifurcation in (5). We then followed the resulting limit cycle branch as A was varied; in all cases, the branch terminates at a homoclinic solution. The results are most conveniently illustrated by plotting the region within the A–c plane in which pattern solutions exist, which is bounded by loci of Hopf bifurcation points and homoclinic solutions. The latter boundary is actually the union of loci of two

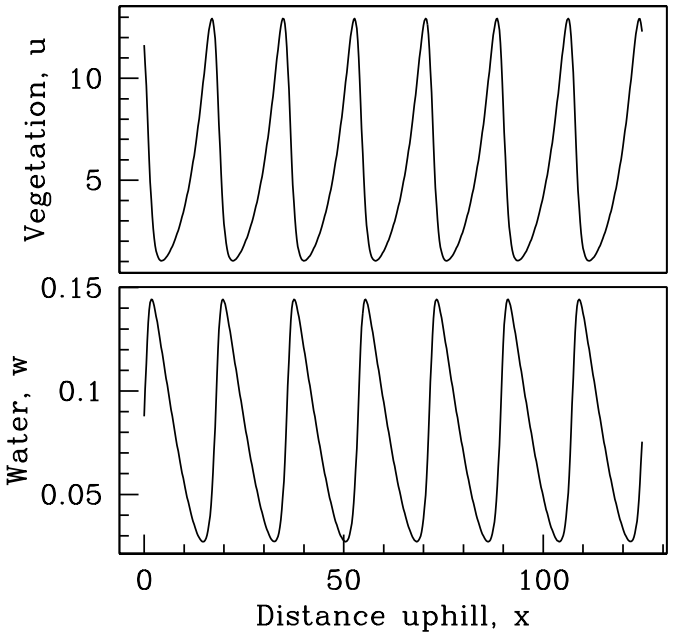

FIGURE 1. An illustration of a pattern solution of (3), showing repeated peaks of vegetation biomass u separated by regions of almost bare ground. There is a corresponding pattern of water w. The pattern moves in the positive x direction (uphill) at a constant speed of about 0.9. The equations were solved numerically on the domain $0 < x < 125$ with periodic boundary conditions, using a semi-implicit finite difference scheme with upwinding for the convective term. The initial conditions ($t = 0$) were small randomly generated perturbations to (u_s, w_s), and the solution is plotted at $t = 8000$. The parameter values are $A = 2.5$, $B = 0.45$, $\nu = 182.5$ and $p = 2.2$.

different homoclinic solutions, which are homoclinic to $(0, A)$ in one case and to the vegetated steady state with $u < u_{min}$ in the other. Figure 2 shows the pattern regions for four different values of p, with $B = 0.45$ and $\nu = 200$ in each case. They have a characteristic shape, with a wide area topped by a thin "tusk-shaped" part; a detailed analytical description of the latter, for $p = 2$, is given in [40, 41, 42].

From the viewpoint of applications, the most significant aspect of Figure 2 is that the range of values of A over which patterns exist decreases markedly as p increases. The maximum value of A for which there are patterns corresponds to a fold in the Hopf bifurcation locus, while the minimum value corresponds to a fold in the locus of solutions homoclinic to $(0, A)$. We tracked these folds numerically as A, c and p were varied simultaneously. As discussed in §1, to obtain results that can be interpreted directly in terms of rainfall variation, it is necessary to calculate ratios of critical values of A. Therefore in Figure 3 we plot, against p, the values of A on these two folds divided by the reference value A_{crit}; recall that this is the minimum value of A for which (u_s, w_s) exists. Patterns occur for ratios of these critical

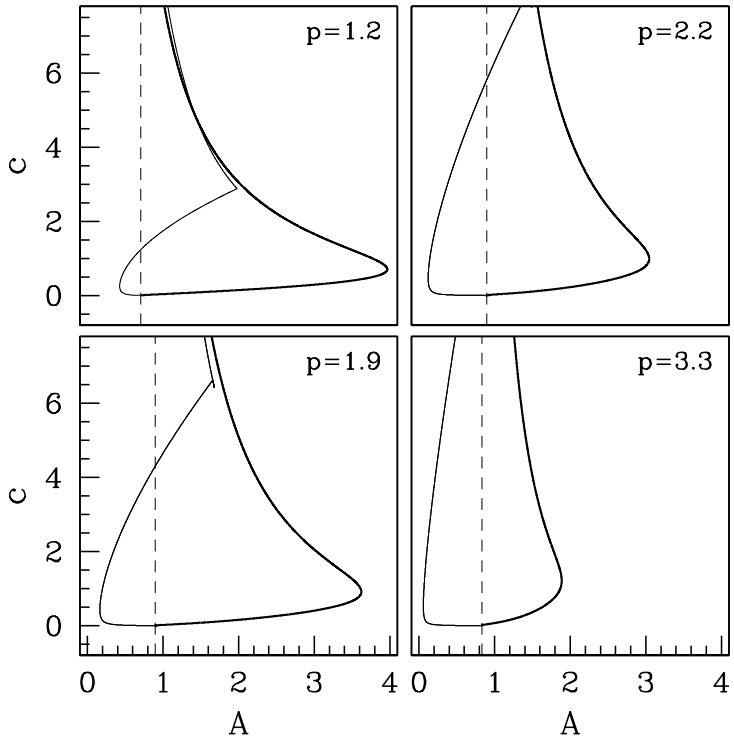

FIGURE 2. Examples of regions in the A (rainfall) – c (wave speed) parameter plane in which (5) has limit cycle solutions, which correspond to pattern solutions of (3). The thick curves are loci of Hopf bifurcations of (u_s, w_s), and the thin curves are loci of homoclinic solutions. In fact we do not calculate actual homoclinic loci; rather, the curves are the loci of solutions with a fixed, large period (2000). The vertical dashed lines show the values of A_{crit}; for $A < A_{crit}$ the steady state (u_s, w_s) does not exist. Limit cycles (patterns) exist between the thick and thin curves. In fact the pattern region is slightly larger than this in the "tusk-shaped" part of the pattern region. Here the thin and thick curves cross; this is visible in the $p = 1.2$ case, but is outside the plot region in the other three cases. In the vicinity of this crossing, the pattern region is bounded on one side by the locus of a fold in the limit cycle branch; details of this for the case $p = 2$ are given in [41]. Computations were done using the software package AUTO [10, 11, 12]. The parameter values are $B = 0.45$ and $\nu = 200$; the values of p are shown in the four panels.

rainfall levels lying between the two curves in Figure 3. Intuitively, smaller rainfall levels are not sufficient to support vegetation, resulting in a full-blown desert, while sufficiently high rainfall permits spatially homogeneous vegetation. Note that the rainfall range giving patterns shrinks to zero as p decreases to 1; this is as expected

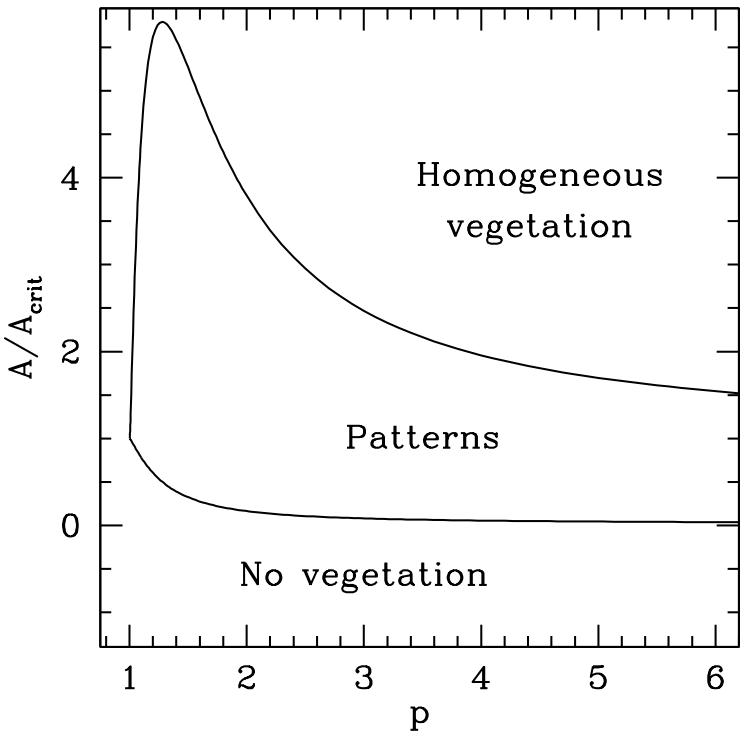

FIGURE 3. An illustration of the rainfall range within which (3) has pattern solutions, for plant loss $B = 0.45$. The upper curve is the locus of folds in the Hopf bifurcation locus, and the lower curve is the locus of folds in the homoclinic solution locus (see Figure 2). In both cases we plot the value of A divided by A_{crit}, which is the minimum value of A for which steady states with $u \neq 0$ exist. These ratios are the same as the ratios of the corresponding critical values of the dimensional rainfall parameter k_4. Computations were done using the software package AUTO [10, 11, 12].

intuitively, since a biomass-dependent infiltration rate is an essential ingredient for pattern formation.

3. **Vegetation boundaries on flat ground.** We continue our investigation into the effects of changing the parameter p by considering a second solution type: interfaces between vegetation and bare ground ("desert") on flat terrain. Therefore we set $\nu = 0$ and consider solutions of (3) satisfying $(u, w) \to (0, A)$ and (u_s, w_s) as $x \to \pm\infty$; note that (u_s, w_s) is always stable when $\nu = 0$. Interface solutions of this type are relevant to desertification [31]. This is a multi-factorial process, but water redistribution is thought to be a significant contributor [22, 37, 53]. Therefore (3) is a relevant model, focussing on one specific aspect of a highly complex problem; for more comprehensive models see for example [16, 22, 36, 54].

Figure 4 shows the solution of (3) for initial conditions consisting of $(u, w) = (u_s, w_s)$ in one half of a large domain, and $(u, w) = (0, A)$ in the other half. The

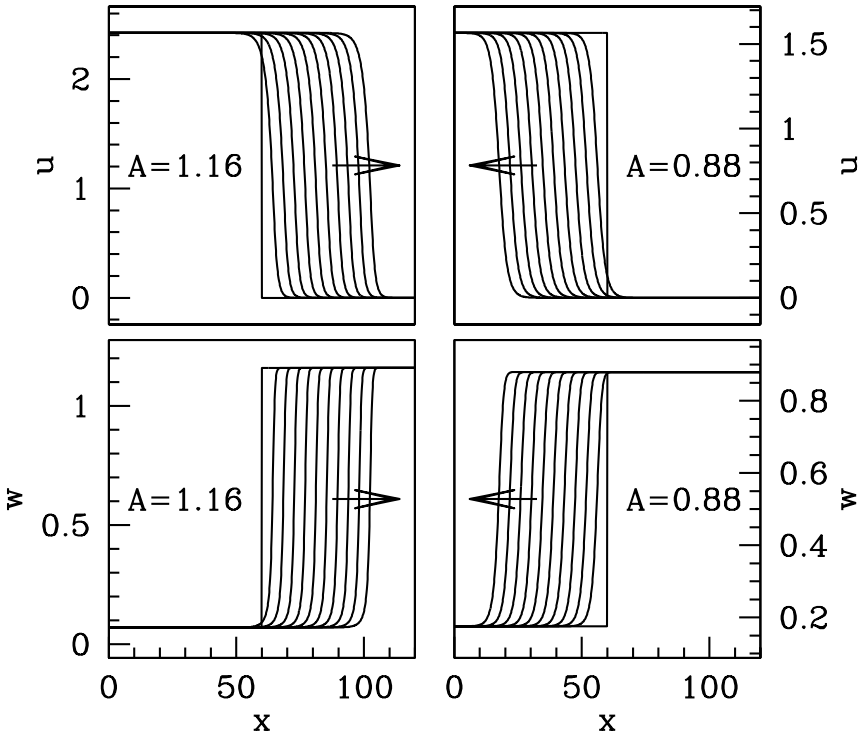

FIGURE 4. Two examples of moving interfaces between vegetation and bare ground in the model (3). We plot vegetation biomass u and water w as a function of space x at times $t = 0, 12, 24, 36, \ldots, 120$ for two values of A, both above A_{crit}. At $t = 0$ we impose $(u, w) = (0, A)$ for $x \leq 60$ and $(u, w) = (u_s, w_s)$ for $x > 60$. In both cases these initial conditions rapidly evolve towards a wave front moving with constant shape and speed. For $A = 1.16$ wave moves in the positive x direction, so that the vegetated region expands; for $A = 0.88$ the opposite applies. The other parameter values are $B = 0.45$, $\nu = 200$ and $p = 3.1$, which imply $A_{crit} \approx 0.844$. The equations were solved using a semi-implicit Crank-Nicolson scheme, and we applied the Dirichlet boundary conditions $(u, w) = (0, A)$ at $x = 0$ and $(u, w) = (u_s, w_s)$ at $x = 120$.

abrupt initial interface smooths out, and then propagates in either the positive or negative x direction, depending on the rainfall parameter A; these behaviours correspond in a very crude way to the expansion and contraction of a desert.

Numerical simulations such as those illustrated in Figure 4 move with constant shape and speed, after initial transients have disappeared. Therefore we consider again travelling wave solutions $(u(x,t), w(x,t)) = (\widetilde{U}(z), \widetilde{W}(z))$ with $z = x - ct$. Our objective is to determine values of the rainfall parameter A for which there is a transition between travelling wave solutions with $c > 0$ and $c < 0$. Such a critical value of A is characterised by the existence of a stationary interface solution.

Therefore we set $c = 0$ (and $\nu = 0$) in the travelling wave equations (5), giving

$$\begin{aligned} d^2\widetilde{U}/dz^2 + \widetilde{W}\widetilde{U}^p - B\widetilde{U} &= 0 \\ A - \widetilde{W} - \widetilde{W}\widetilde{U}^p &= 0 \end{aligned} \tag{6}$$

from which $\widetilde{W}$ can be elimiated:

$$d^2\widetilde{U}/dz^2 + A\widetilde{U}^p/(1+\widetilde{U}^p) - B\widetilde{U} = 0 \tag{7}$$

Multiplying (7) by $d\widetilde{U}/dz$ and integrating gives

$$\left(\frac{d\widetilde{U}}{dz}\right)^2 + 2A\int_{\xi=0}^{\xi=\widetilde{U}} \frac{\xi^p}{1+\xi^p}\,d\xi - B\widetilde{U}^2 = K \tag{8}$$

where K is a constant of integration. We require $d\widetilde{U}/dz = 0$ when $\widetilde{U} = 0$ and $\widetilde{U} = u_s$, so that $K = 0$ and

$$A/B = \tfrac{1}{2}u_s^2\left[\int_{\xi=0}^{\xi=u_s} \frac{\xi^p}{1+\xi^p}\,d\xi\right]^{-1}. \tag{9}$$

Since (u_s, w_s) is a homogeneous steady state of (3) with $u \neq 0$, u_s satisfies (4), i.e.

$$u_s + u_s^{1-p} = A/B\,. \tag{10}$$

Equations (9) and (10) together determine values of A for which there is a stationary interface solution of (3). In practice it is most convenient to combine (9) and (10) into a single equation for u_s:

$$\Phi(u_s) \equiv 2\int_{\xi=0}^{\xi=u_s} \frac{1}{1+\xi^p}\,d\xi - \left[\frac{u_s(2+u_s^p)}{1+u_s^p}\right] = 0\,. \tag{11}$$

Then

$$\Phi'(u_s) = \frac{u_s^p\,(p-1-u_s^p)}{(1+u_s^p)^2}$$

so that Φ is strictly increasing on $(0, u_{min})$ and strictly decreasing on (u_{min}, ∞). (Recall that $u_{min} = (p-1)^{1/p}$). Moreover $\Phi(0) = 0$, so that $\Phi(u_{min}) > 0$. As $u_s \to \infty$, the integral in (11) remains finite, while the term in square brackets $\to \infty$, implying that $\Phi(u_s) < 0$ for sufficiently large u_s. Therefore (11) has exactly one solution for u_s on (u_{min}, ∞), and (10) implies that there is exactly one value of A corresponding to this solution. For this value of A, (6) and (8, with $K = 0$) then imply existence and uniqueness of a stationary interface solution, up to orientation reversal and translation. Figure 5 shows the value of A giving this stationary interface as a function of p. As discussed in §1, we plot A/A_{crit} on the vertical axis; this can be directly interpreted as the ratio of the corresponding critical values of the dimensional rainfall parameter k_4.

4. **Discussion.** In semi-arid environments, the infiltration capacity of soil is dependent on vegetation biomass. In this paper we have studied the way in which the strength of this dependence affects the formation of banded vegetation patterns on slopes, and the movement of boundaries between vegetation and bare ground on flat terrain. Our key results are Figures 3 and 5; respectively, these figures show how changes in the strength of the dependence of infiltration capacity on biomass alter the rainfall range over which patterns occur, and the rainfall level above which vegetated regions expand into adjacent desert.

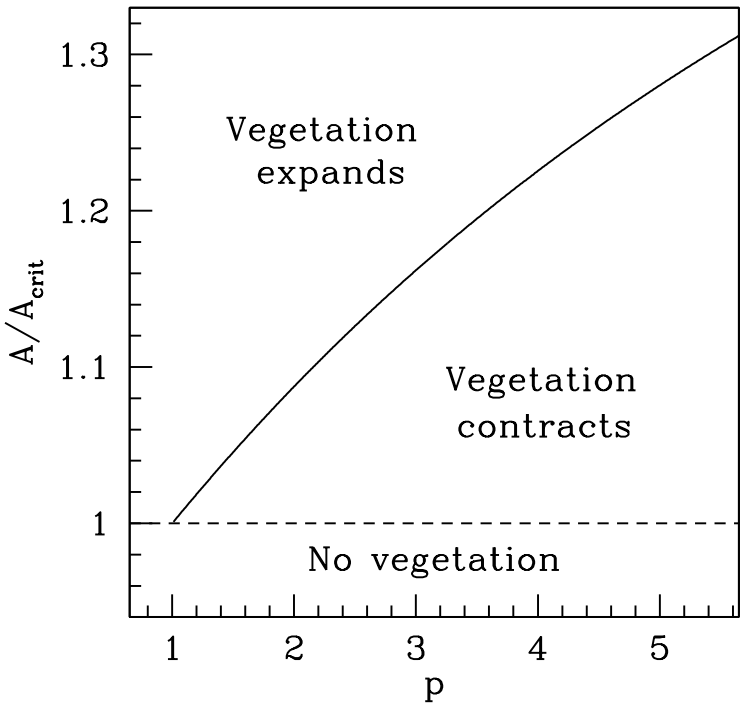

FIGURE 5. An illustration of the rainfall level at which interfaces between vegetation and bare ground change their direction of movement (solid curve), calculated by solving (11) for u_s and then using (10) to obtain the corresponding value of A. We plot the value of A divided by A_{crit}, which is the minimum value of A for which steady states with $u \neq 0$ exist. This ratio is the same as the ratio of the corresponding critical values of the dimensional rainfall parameter k_4. The dashed line is simply $A = A_{crit}$.

Our work raises a number of mathematical issues that are natural targets for future research, amongst which we regard two as being of particular importance.

1. *Pattern selection:* We have shown that, for a given value of A within the pattern forming range, patterns exist for a range of values of the wave speed c. Therefore a key question is: what wave speed is selected by given initial and boundary conditions? A previous numerical study for the Klausmeier model ($p = 2$) suggests that wave selection is history dependent [39] and a detailed analytical investigation of this is an important challenge for future work. This issue is closely associated with wave stability; no analytical results on this are available, but an approximate numerical study is presented in [39].
2. *Existence and uniqueness of wave fronts:* Numerical simulations of (3) suggest that for any given values of B, p and $A > A_{crit}$, with $\nu = 0$, there is exactly one travelling wave front solution connecting the stable steady states $(u, w) = (0, A)$ and $(u, w) = (u_s, w_s)$. Figure 6 illustrates the variation with A of the numerically calculated wave speed, for one pair of B and p values. Existence and uniqueness of travelling waves in scalar reaction-diffusion

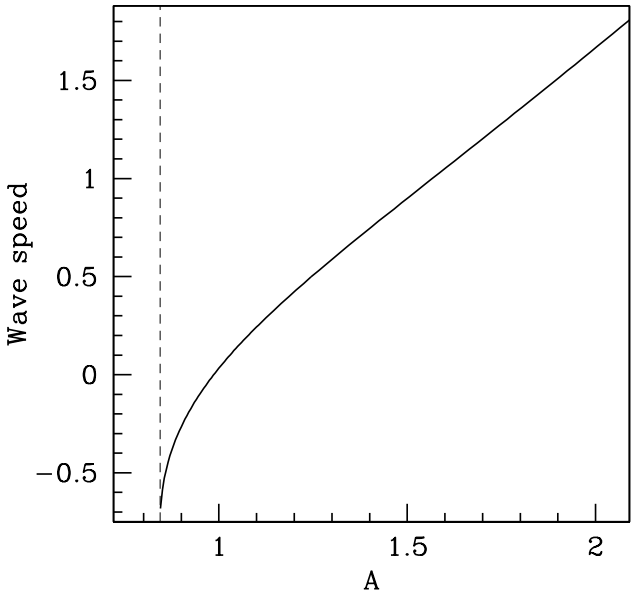

FIGURE 6. The variation with the rainfall parameter A of the speed of interfaces between vegetation and bare ground. Two examples of such moving interfaces are shown in Figure 4, and the other parameter values are the same as in that figure. The vertical dashed line indicates the value of $A_{crit} \approx 0.844$. We solved up to $t = 108$ on the domain $0 < x < 840$, with initial conditions ($t = 0$) $(u, w) = (0, A)$ for $x \leq 420$ and $(u, w) = (u_s, w_s)$ for $x > 420$. We applied the Dirichlet boundary conditions $(u, w) = (0, A)$ at $x = 0$ and $(u, w) = (u_s, w_s)$ at $x = 840$. The wave speed was calculated via the distance travelling by the front during $60 \leq t \leq 108$. The equations were solved using a semi-implicit Crank-Nicolson scheme, with grid spacing 0.12 and time step 0.002. Detailed numerical convergence tests show that these give an error in the wave speed of $1.4 \times 10^{-4} \approx 0.04\%$ for $A = 0.88$, and $5.4 \times 10^{-3} \approx 0.3\%$ for $A = 2.2$.

equations with bistable kinetics was proved more than 30 years ago [15]. For systems, a corresponding general result applies when the diffusion matrix is diagonal with strictly positive diagonal entries, and when the kinetics are locally monotone [51, Theorem 1.1 of Chapter 3]. However there are only a very few results (e.g. [9]) for non-monotone systems. For "degenerate" monotone systems, in which one diffusion coefficient is zero, there are a number of recent results (e.g. [2, 14, 21]), but no general theory. Our system (3) is both non-monotone and degenerate, so that proving existence and uniqueness of travelling waves is a major but important challenge for the future.

Acknowledgments. JAS thanks Yaping Wu (Capital Normal University, Beijing) for discussions that initiated the work in §3 of this paper.

REFERENCES

[1] M. R. Agular and O. E. Sala, *Patch structure, dynamics and implications for the functioning ofarid ecosystems*, Trends Ecol. Evol., **14** (1999), 273–277.

[2] E. O. Alzahrani, F. A. Davidson and N. Dodds, *Travelling waves in near-degenerate bistable competition models*, Math. Model. Nat. Phenom., **5** (2010), 13–35.

[3] N. Barbier, P. Couteron, R. Lefever, V. Deblauwe and O. Lejeune, *Spatial decoupling of facilitation, competition at the origin ofgapped vegetation patterns*, Ecology, **89** (2008), 1521–1531.

[4] S. S. Berg and D. L. Dunkerley, *Patterned mulga near Alice Springs, central Australia, and thepotential threat of firewood collection on this vegetation community*, J. Arid Environ., **59** (2004), 313–350.

[5] A. I. Borthagaraya, M. A. Fuentesa and P. A. Marque, *Vegetation pattern formation in a fog-dependent ecosystem*, J. Theor. Biol., **265** (2010), 18–26.

[6] R. M. Callaway, *Positive interactions among plants*, Botanical Rev., **61** (1995), 306–349.

[7] P. Couteron, A. Mahamane, P. Ouedraogo and J. Seghieri, *Differences between banded thickets (tiger bush) at two sites in West Africa*, J. Veg. Sci., **11** (2000), 321–328.

[8] V. Deblauwe, P. Couteron, J. Bogaert and N. Barbier, *Determinants and dynamics of banded vegetation pattern migration in arid climates*, Ecological monographs, **82** (2012), 3–21.

[9] J. D. Dockery and R. Lui, *Existence of traveling wave solutions for a bistable evolutionary ecology model*, SIAM J. Math. Anal., **23** (1992), 870–888.

[10] E. J. Doedel, *AUTO: A program for the automatic bifurcation analysis of autonomous systems*, Cong. Numer., **30** (1981), 265–284.

[11] E. J. Doedel, H. B. Keller and J. P. Kernévez, *Numerical analysis and control of bifurcation problems. I. Bifurcation in finite dimensions*, Int. J. Bifurc. Chaos Appl. Sci. Engrg., **1** (1991), 493–520.

[12] E. J. Doedel, W. Govaerts, Yu. A. Kuznetsov and A. Dhooge, *Numerical continuation of branch points of equilibria and periodic orbits*, Internat. J. Bifur. Chaos Appl. Sci. Engrg., **15** (2005), 841–860.

[13] D. L. Dunkerley and K. J. Brown, *Oblique vegetation banding in the Australian arid zone: Implications for theories of pattern evolution and maintenance*, J. Arid Environments, **52** (2002), 163–181.

[14] J. Fang and X.-Q. Zhao, *Monotone wavefronts for partially degenerate reaction-diffusion systems*, J. Dyn. Diff. Eq., **21** (2009), 663–680.

[15] P. C. Fife and J. B. McLeod, *The approach of solutions of nonlinear diffusion equations to travelling front solutions*, Arch. Rat. Mech. Anal., **65** (1977), 335–361.

[16] A. Giannini, M. Biasutti and M. M. Verstraete, *A climate model-based review of drought in the Sahel: Desertification, the re-greening and climate change*, Global Planet. Change, **64** (2008), 119–128.

[17] E. Gilad, J. von Hardenberg, A. Provenzale, M. Shachak and E. Meron, *A mathematical model of plants as ecosystem engineers*, J. Theor. Biol., **244** (2007), 680–691.

[18] V. Guttal and C. Jayaprakash, *Self-organisation and productivity in semi-arid ecosystems: Implications of seasonality in rainfall*, J. Theor. Biol., **248** (2007), 290–500.

[19] R. HilleRisLambers, M. Rietkerk, F. van de Bosch, H. H. T. Prins and H. de Kroon, *Vegetation pattern formation in semi-arid grazing systems*, Ecology, **82** (2001), 50–61.

[20] R. C. Hills, *The influence of land management and soil characteristics on infiltration and the occurrence of overland flow*, J. Hydrology, **13** (1971), 163–181.

[21] Y. Jin and X.-Q. Zhao, *Bistable waves for a class of cooperative reaction-diffusion systems*, J. Biol. Dyn., **2** (2008), 196–207.

[22] S. Kéfi, M. Rietkerk, C. L. Alados, Y. Pueyo, A. ElAich, V. Papanastasis and P. C. de Ruiter, *Spatial vegetation patterns and imminent desertification in Mediterranean arid ecosystems*, Nature, **449** (2007), 213–217.

[23] S. Kéfi, M. Rietkerk and G. G. Katul, *Vegetation pattern shift as a result of rising atmospheric CO2 in arid ecosystems*, Theor. Pop. Biol., **74** (2008), 332–344.

[24] C. A. Klausmeier, *Regular and irregular patterns in semiarid vegetation*, Science, **284** (1999), 1826–1828.

[25] A. Y. Kletter, J. von Hardenberg, E. Meron and A. Provenzale, *Patterned vegetation and rainfall intermittency*, J. Theor. Biol., **256** (2009), 574–583.

[26] R. Lefever and O. Lejeune, *On the origin of tiger bush*, Bull. Math. Biol., **59** (1997), 263–294.

[27] R. Lefever, N. Barbier, P. Couteron and O. Lejeune, *Deeply gapped vegetation patterns: On crown/root allometry, criticality and desertification*, J. Theor. Biol., **261** (2009), 194–209.
[28] W. MacFadyen, *Vegetation patterns in the semi-desert plains of British Somaliland*, Geographical J., **115** (1950), 199–211.
[29] A. K. McDonald, R. J. Kinucan and L. E. Loomis, *Ecohydrological interactions within banded vegetation in the northeastern Chihuahuan Desert, USA*, Ecohydrology, **2** (2009), 66–71.
[30] C. Montaña, *The colonization of bare areas in two-phase mosaics of an arid ecosystem*, J. Ecol., **80** (1992), 315–327.
[31] E. N. Mueller, J. Wainwright and A. J. Parsons, *The stability of vegetation boundaries and the propagation ofdesertification in the American Southwest: A modelling approach*, Ecol. Model., **208** (2007), 91–101.
[32] Y. Pueyo, S. Kéfi, C. L. Alados and M. Rietkerk, *Dispersal strategies and spatial organization of vegetation in arid ecosystems*, Oikos, **117** (2008), 1522–1532.
[33] M. Rietkerk, P. Ketner, J. Burger, B. Hoorens and H. Olff, *Multiscale soil and vegetation patchiness along a gradient of herbivore impact in a semi-arid grazing system in West Africa*, Plant Ecology, **148** (2000), 207–224.
[34] M. Rietkerk, M. C. Boerlijst, F. van Langevelde, R. HilleRisLambers, J. van de Koppel, H. H. T. Prins and A. de Roos, *Self-organisation of vegetation in arid ecosystems*, Am. Nat., **160** (2002), 524–530.
[35] M. Rietkerk, S. C. Dekker, P. C. de Ruiter and J. van de Koppel, *Self-organized patchiness and catastrophic shifts in ecosystems*, Science, **305** (2004), 1926–1929.
[36] T. M. Scanlon, K. K. Caylor, S. A. Levin and I. Rodriguez-Iturbe, *Positive feedbacks promote power-law clustering of Kalahari vegetation*, Nature, **449** (2007), 209–212.
[37] W. H. Schlesinger, J. F. Reynolds, G. L. Cunningham, L. F. Huenneke, W. M. Jarrell, R. A. Virginia and W. G. Whitford, *Biological feedbacks in global desertification*, Science, **247** (1990), 1043–1048.
[38] J. A. Sherratt, *An analysis of vegetation stripe formation in semi-arid landscapes*, J. Math. Biol., **51** (2005), 183–197.
[39] J. A. Sherratt and G. J. Lord, *Nonlinear dynamics, pattern bifurcations in a model for vegetation stripes in semi-arid environments*, Theor. Pop. Biol., **71** (2007), 1–11.
[40] J. A. Sherratt, *Pattern solutions of the Klausmeier model for banded vegetationin semi-arid environments I*, Nonlinearity, **23** (2010), 2657–2675.
[41] J. A. Sherratt, *Pattern solutions of the Klausmeier model for banded vegetationin semi-arid environments II. Patterns with the largest possible propagation speeds*, Proc. R. Soc. Lond. A, **467** (2011), 3272–3294.
[42] J. A. Sherratt, *Pattern solutions of the Klausmeier model for banded vegetationin semi-arid environments III. The transition between homoclinic solutions*, submitted.
[43] G.-Q. Sun, Z. Jin and Q. Tan, *Measurement of self-organization in arid ecosystems*, J. Biol. Systems, **18** (2010), 495–508.
[44] D. J. Tongway and J. A. Ludwig, *Theories on the origins, maintainance, dynamics, and functioning ofbanded landscapes*, in "Banded Vegetation Patterning in Arid and Semi-Arid Environments"(eds. D. J. Tongway, C. Valentin and J. Seghieri), Springer, New York, (2001), 20–31.
[45] N. Ursino and S. Contarini, *Stability of banded vegetation patterns under seasonal rainfall and limited soil moisture storage capacity*, Adv. Water Resour., **29** (2006), 1556–1564.
[46] N. Ursino, *Modeling banded vegetation patterns in semiarid regions: Inter-dependence between biomass growth rate and relevant hydrological processes*, Water Resour. Res., **43** (2007), W04412.
[47] N. Ursino, *Above and below ground biomass patterns in arid lands*, Ecol. Model., **220** (2009), 1411–1418.
[48] C. Valentin, J. M. d'Herbès and J. Poesen, *Soil and water components of banded vegetation patterns*, Catena, **37** (1999), 1–24.
[49] C. Valentin and J. M. d'Herbès, *Niger tiger bush as a natural water harvesting system*, Catena, **37** (1999), 231–256.
[50] J. van de Koppel, M. Rietkerk, F. van Langevelde, L. Kumar, C. A. Klausmeier, J. M. Fryxell, J. W. Hearne, J. van Andel, N. de Ridder, M. A. Skidmore, L. Stroosnijder and H. H. T. Prins, *Spatial heterogeneity and irreversible vegetation change in semiarid grazing systems*, Am. Nat., **159** (2002), 209–218.

[51] A. I. Volpert, V. A. Volpert and V. A. Volpert, "Travelling Wave Solutions of Parabolic Systems," Translations of Mathematical Monographs, **140**, American Mathematical Society, Providence, RI, 1994.

[52] J. von Hardenberg, A. Y. Kletter, H. Yizhaq, J. Nathan and E. Meron, *Periodic versus scale-free patterns in dryland vegetation*, Proc. R. Soc. Lond. B, **277** (2010), 1771–1776; American Mathematical Society, Providence RI, 1994.

[53] M. Yu, Q. Gao, H. E. Epstein and X. S. Zhang, *An ecohydrological analysis for optimal use of redistributed water among vegetation patches*, Ecol. Appl., **18** (2008), 1679–1688.

[54] N. Zeng and J. Yoon, *Expansion of the world's deserts due to vegetation-albedo feedback under global warming*, Geophys. Res. Lett., **36** (2009), art. no. L17401.

Received March 2011; revised August 2011.

E-mail address: jas@ma.hw.ac.uk
E-mail address: a.d.synodinos@gmail.com